J Mater Sci (2018) 53:14598–14607

Energy materials

Structural supercapacitors using a solid resin electrolyte with carbonized electrospun cellulose/carbon nanotube electrodes

Qiang Li[1], Yanqiu Q. Zhu[1], and Stephen J. Eichhorn[2,*]

[1] College of Engineering, Maths and Physical Sciences, University of Exeter, North Park Road, Exeter, Devon EX4 4QF, UK
[2] Bristol Composites Institute (ACCIS), School of Civil, Aerospace and Mechanical Engineering, University of Bristol, University Walk, Bristol BS8 1TR, UK

Received: 11 April 2018
Accepted: 4 July 2018
Published online: 17 July 2018

ABSTRACT

Novel cellulose-derived hybrid carbon nanofibre (CNF)/carbon nanotubes (CNTs) electrode-based structural supercapacitors, combined with a solid electrolyte, have been produced. Galvanostatic charge/discharge and electrochemical impedance spectroscopy measurements were used to assess the electrodes' performance. The CNF/CNTs electrodes have a better capacitive performance than the plain CNF electrodes; 0.91 ± 0.02 and 3.35 ± 0.05 mF cm^{-2} for CNF and CNF/CNTs, respectively. A Raman spectroscopic approach was used to investigate the stress transfer properties of the CNF within a poly(methyl methacrylate) (PMMA) resin matrix. Deformation of the carbon structures was observed via shifts towards a lower wavenumber position of the G band ($\sim$ 1590 cm^{-1}) for CNF and CNF/CNTs samples processed at a carbonization temperature of 2000 °C. Moduli of these fibres were estimated to be $\sim$ 145 and $\sim$ 271 GPa, respectively, suggesting the growth of CNTs not only enhances the capacitive performance but also the mechanical performance of the structural supercapacitors.

Introduction

Supercapacitors are energy storage devices that have high power densities and long lifetimes compared with batteries [1]. Charge storage in supercapacitors takes advantage of the electrostatic field that forms at the electrolyte/electrode interface [2]. Novel strategies to fabricate so-called multifunctional structural supercapacitors have been of interest in recent years [3]. Structural supercapacitors generally make use of an electrode, a solid electrolyte and a separator that simultaneously resist mechanical stresses and store electrochemical energy [3]. Among the materials used for electrodes in structural supercapacitors, carbon fibres are one of the best candidates, since they combine both conductive and high mechanical properties (stiffness, strength) for reinforcing matrix electrolytes [4].

Address correspondence to E-mail: s.j.eichhorn@bristol.ac.uk

https://doi.org/10.1007/s10853-018-2665-x

Recently, electrospinning has been applied to prepare nanofibres for electrocapacitive applications [5]. This approach can be used to spin precursor materials, which when thermally treated can be converted to carbon nanofibre (CNF)-based electrodes [6]. These electrodes can be used for supercapacitors, due to their high surface area to volume ratios, desirable porosity, and excellent mechanical properties [7]. We have recently shown that carbon nanotubes (CNTs) can be grown on the surface of carbon fibres, produced by an electrospinning method, improving the electrocapacitive performance [8]. Growing CNTs on the surface of the carbon fibres could also be an effective approach to enhance the interfacial strength of a structural supercapacitor, as has been shown to be the case with traditional composite materials [9, 10].

The stress transfer efficiency between carbon fibres and a matrix is one of the most important properties of a composite in terms of its mechanical performance. An interface with high-stress transfer efficiency allows stress to be transferred to the reinforcing phase. The stress transfer depends on the interfacial shear stress between the fibre and the matrix [11]. Qian et al. evaluated the in-plane shear properties of carbon aerogel-modified carbon fibre fabric-based structural supercapacitors using the ASTM standard D3518 [12]. Over the years Raman spectroscopy has been successfully applied to evaluate the mechanical properties of carbon materials by the observation of the shift in the position of characteristic bands when the materials are deformed [13]. This technique was initially developed by Young and co-workers for the deformation of carbon fibres [14]. Since then, it has been applied to investigate the mechanical properties of other carbon materials such as CNTs [15] and graphene [16]. The Raman shift arises from the change of vibrational frequencies of the normal modes when deformation is applied [11]. It is believed that an increase in the stress transfer from the matrix to the carbon fibres results in a larger Raman band shift [17]. Raman spectroscopy also has been reported as a technique to estimate the mechanical stiffness of CNFs produced from electrospun precursors [6].

In the present study, a structural supercapacitor is produced by a hierarchical construction of CNFs. These CNFs are decorated with CNTs for use as electrode materials. These electrodes are combined with poly(ethylene glycol) diglycidyl ether (PEGDGE), which acts as both a solid polymer electrolyte and a matrix material. Raman spectroscopy is used to assess the mechanical properties of these fibres, and their appropriateness for a structural supercapacitor.

Experimental methods

Production of structural supercapacitors

Electrodes were prepared by carbonization of electrospun de-acetylated cellulose acetate fibres at a temperature of 900 °C, followed by CVD to generate CNTs, and finally a KOH activation of their surface. A full description of the production of these fibres from cellulose acetate precursor is contained within a previous publication [8]. Plain carbon fibres and CNTs decorated filaments are subsequently denoted as CF900 and CF900/CNTs, respectively. Carbon fibres produced at temperatures of 1500 and 2000 °C are denoted as CF1500 and CF2000, and their respective CNTs decorated samples as CF1500/CNTs and CF2000/CNTs.

1-ethyl-3-methylimidazolium bis(trifluoromethylsulfonyl) imide (EMITFSI, purity $\geqslant$ 98%), PEGDGE (Mn $\sim$ 500), and triethylenetetramine (TETA) were purchased from Sigma-Aldrich (Dorset, UK). Solid electrolyte was prepared by mixing 10 wt% EMITFSI as an ionic liquid in an 82.6 wt% PEGDGE-based epoxy resin, followed by magnetic stirring for 5 min. TETA at 7.4 wt% was used as a hardener, and added to the mixed PEGDGE/EMITFSI solution, followed by manually stirring for 12 min until a homogeneous solution was obtained. The mixed PEGDGE/EMITFSI/TETA solution of 0.25 ml was then deposited onto a 13 × 13 mm^2 Whatman glass fibre separator. Activated CF900 or CF900/CNTs fibrous networks were weighed (to 2.2 mg) and then deposited on each side of the separator. Two copper tape current collectors were cut into 45 mm × 10 mm × 0.3 mm shapes and firmly attached on both sides of the electrode layers. The supercapacitors were then placed into an oven at 80 °C for curing. The curing durations were 2 and 24 h for comparison, during which the supercapacitors were pressed under a load of 10 kg to fasten them. A schematic of a structural supercapacitor produced using this method is shown in Fig. 1.

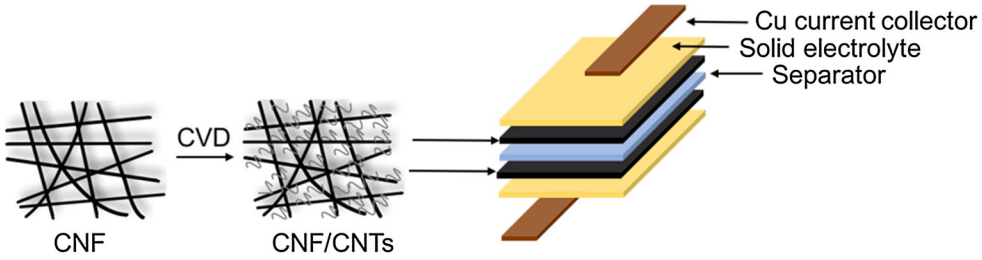

Figure 1 Schematic of a structural supercapacitor based on CNF/CNTs electrodes, a glass fibre separator and a solid electrolyte.

Preparation of in situ deformation samples

For in situ Raman spectroscopy studies, a 5 mm × 5 mm square sample of the CF900 or CF900/CNTs material was placed centrally on a 70 mm × 22 mm × 1.5 mm PMMA beam. Two drops (0.25 mL) of the PEGDGE/EMITFSI/TETA resin were deposited on top of the samples. The PMMA beam with this resin was heat cured in an oven at 80 °C for 2 and 24 h. The samples were then removed from the oven and cooled in air.

CF1500, CF1500/CNTs, CF2000 and CF2000/CNTs samples were fabricated for mechanical properties characterization. Instead of making structural supercapacitors using the solid electrolyte, PMMA/CNF/PMMA or PMMA/CNF/CNTs/PMMA composites were prepared for in situ Raman spectroscopy/bending tests. CF1500, CF1500/CNTs, CF2000 or CF2000/CNTs samples were placed centrally on PMMA beams. Two drops (0.25 mL) of 0.1 g ml^{-1} PMMA/acetone solution were then deposited over this sample and dried at room temperature for 1 h.

Characterization of materials

A scanning electron microscope (SEM) (HITACHI S3200 N SEM–EDS) with a voltage of 20 kV was used to observe the morphologies of the CNF and the CNF/CNTs. The specific surface area was calculated by the Brunauer–Emmett–Teller (BET) method using a Micromeritics ASAP 2020 device.

Galvanostatic charge and discharge (GCD) curves were obtained at a current density of 38 μA cm^{-2} after 2 h of curing. Electrochemical impedance spectra (EIS) were obtained at a constant perturbation amplitude of 5 mV within a frequency range 0.01 to 10^6 Hz after both 2 and 24 h of curing.

A Renishaw RM1000 Raman spectrometer coupled to an Ar laser (λ = 532 nm), and a Leica CC detector, recorded spectra from the samples during in situ deformation of the samples. The laser spot size was ~ 1 to 2 μm, and the focused power was ~ 1 mW when using a 50 × objective lens. Exposure times to collect spectra between strain increments were 30 s. A strain gauge (type CEA-06-240UZ-120, Vishay Micro-Measurements) was attached to the surface of the PMMA beam using cyanoacrylate adhesive. Two wires were soldered to each copper tab of the strain gauge, which were connected to a transducer. A four-point bending rig was used to deform the samples in tension. Raman spectra were recorded in 0.05% strain intervals up to 0.9% strain.

Results and discussion

Morphology and porosity characterization of CNF and CNF/CNTs

Figure 2a, b shows the morphologies of CF900 and CF900/CNTs, respectively. CNTs were observed at the circumferential surfaces of CF900. No other carbon impurities were observed after CVD, in agreement with a previous study [18]. The absorption–desorption isotherms for these materials and their respective surface areas have been previously reported; surface area was found to grow from 712 to 1211 m^2 g^{-1} after growth of CNTs on CNF [8].

Galvanostatic charge and discharge tests

GCD curves for the CF900 and CF900/CNTs electrodes at a current density of 38 μA cm^{-2} after curing for 2 h are reported in Fig. 3. The specific capacitances of CF900 and CF900/CNTs electrodes are calculated to be 0.91 ± 0.02 mF cm^{-2} (699 ± 15 mF g^{-1} or 114 ± 3 mF cm^{-3}) and 3.35 ± 0.05 mF cm^{-2} (2573 ± 38 mF g^{-1} or 419 ± 6 mF cm^{-3}), respectively. The values of the capacitance are higher than the multiwall CNTs impregnated carbon fibre-based

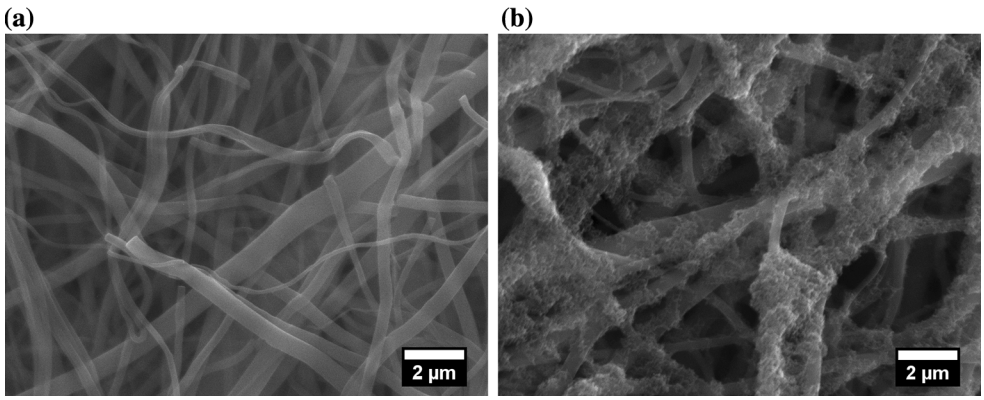

Figure 2 Typical SEM images of **a** CNF and **b** CNF/CNTs samples.

electrodes reported in a recent study [19] and several times higher compared with the specific capacitance (52 mF g^{-1}) for activated carbon fibre electrodes [20]. The large IR drop (a rapid voltage change at the initial stage of the discharge) for both GCD curves indicates that there is large equivalent series resistance (R_s) in the capacitors.

EIS testing of the supercapacitor electrodes

EIS measurements were taken to evaluate the resistive properties of the capacitors, as shown in Fig. 4. The EIS data between 1 and 10^6 Hz were fitted using Zview software based on an equivalent circuit model (inset of Fig. 4). The equivalent series resistance (R_s) was then obtained as the intercept of the real axis within the high-frequency region of the Nyquist plot. The R_s value is the total resistance of the electrode, electrolyte, and the current collector. As shown in Table 1, the R_s value for the CF900 electrode (535 ± 27 Ω) is higher compared to CF900/CNTs (470 ± 21 Ω) after a curing time of 24 h. A higher R_s value is also observed for CF900 after a curing time of 2 h. This indicates that the growth of CNTs increases the electron transport properties of the electrodes. Other than the gel electrolyte itself, this gives rise to a relatively large R_s for all structural capacitors; the use of copper collectors may also be a source of resistance. However, the values of R_s and R_{ct} are significantly lower than reported in recent work in which the structural supercapacitors were made by the same PEGDGE electrolyte/10 wt% EMITFSI with monolithic carbon aerogel-modified carbon fabric electrodes [12]. This shows the CF900 and CF900/CNTs electrodes are competitive in terms of their capacitive performance.

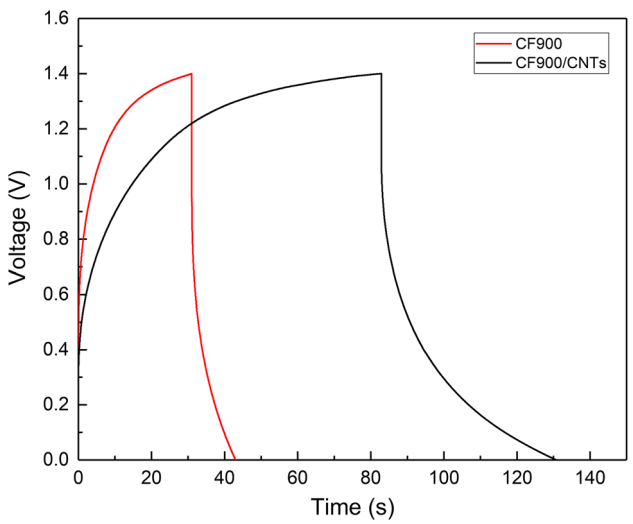

Figure 3 GCD curves for CF900 and CF900/CNTs after curing 2 h.

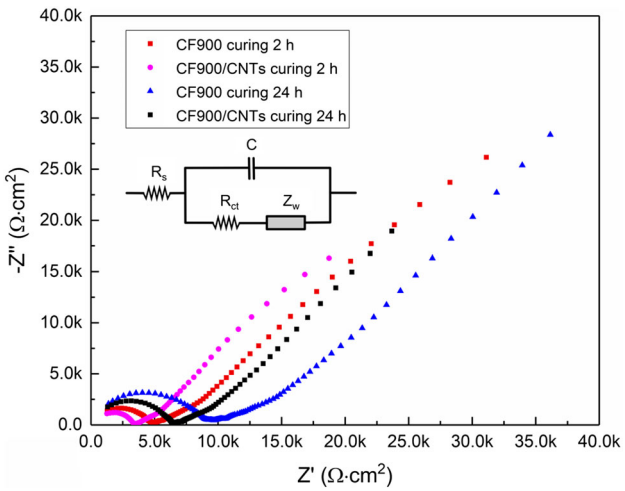

Figure 4 Typical EIS curves for CF900 and CF900/CNTs electrodes after curing for 2 and 24 h. The inset is the equivalent electrical circuit model.

Table 1 The values of R_s and R_{ct} for CF900 and CF900/CNTs after curing for 2 and 24 h

	R_s (2 h) Ω	R_{ct} (2 h) Ω	R_s (24 h) Ω	R_{ct} (24) Ω
CF900	482 ± 19	2014 ± 24	535 ± 27	3502 ± 100
CF900/CNTs	451 ± 13	1471 ± 13	470 ± 21	2909 ± 33

The middle to the high-frequency region of the Nyquist plot, in which the R_{ct} value is obtained from the diameter of the semicircle, illustrates the charge transfer resistance that occurs at the interface between the electrode and electrolyte. The R_{ct} value results from the movement of charge complexes close to the Helmholtz plane [21]. As shown in Table 1, smaller semicircles are observed for CF900/CNTs electrodes after both curing times of 2 and 24 h. This demonstrates that these electrodes have lower interfacial resistance, with better charge transfer behaviour than the CF900 electrodes. In addition, the R_{ct} values for both CF900 and CF900/CNTs electrodes increase after 24 h of curing in comparison to 2 h. This indicates that enhanced curing leads to a reduced charge transfer behaviour. This is thought to be because as the electrolyte becomes more solid, it hinders the charge mobility at the interface between the electrolyte and the electrodes.

The 45° region in the Nyquist plot is known as the Warburg region; the slope of this portion of the curve is called the Warburg resistance (Z_w) and is a result of the frequency dependence of ion diffusion/transport in the electrolyte [22]. In addition, the behaviour of the diffusion of ions in the electrolyte can be characterized by the slope of a regression to the linear region at low-frequency; up to 0.01 Hz in the present work. Normally the vertical line represents the formation of an ideal capacitor. However, the straight lines of all the electrodes have a slope of approximately 45°, showing what could be both kinetic and diffusion-controlled behaviour. Moreover, there is no obvious change in the slope for both CF900 and CF900/CNTs samples (for both the 2 and 24 h curing times), indicating the growth of CNTs does not significantly affect the diffusion of the ions.

Structural features of the electrodes characterized by Raman spectroscopy

Typical Raman spectra obtained from all samples are presented in Fig. 5. These spectra were fitted using two Lorentzian curves to determine the position of the G band, and the intensities of the D and G bands. The intensity ratio of the D and G band (I_D/I_G) with carbonization temperature is reported in Fig. 6. These data show that the I_D/I_G ratio is in the order of CF900 < CF1500 < CF2000.

From previous work by Kong et al. [23], graphitization cannot be achieved at temperatures below ~ 1600 °C, therefore the crystallite size is not expected to be as large as for a fully graphitized structure (L_a> 2 nm) for the CF900 and CF1500 samples. The relationship between I_D/I_G and L_a, therefore, obtained for $L_a < 2$ nm is [8, 24, 25]

$$I_D/I_G = 0.0062L_a^2 \quad (1)$$

In contrast, the crystallite size for the CF2000 sample is thought to be larger than 2 nm. The evolution of disorder is typically quantified using the Tuinstra–Koenig equation [26] described by the equation

$$I_D/I_G = 4.95\,\text{nm}/L_a \quad (2)$$

Therefore, the L_a values for the CF900, CF1500, and CF2000 electrodes are found to be 1.3 ± 0.01, 1.43 ± 0.01 and 2.56 ± 0.04 nm, respectively. In theory, a carbon fibre with a higher lateral crystal size L_a indicates a high degree of graphitization, and thereby an increased grain size results in stronger sp^2 carbon

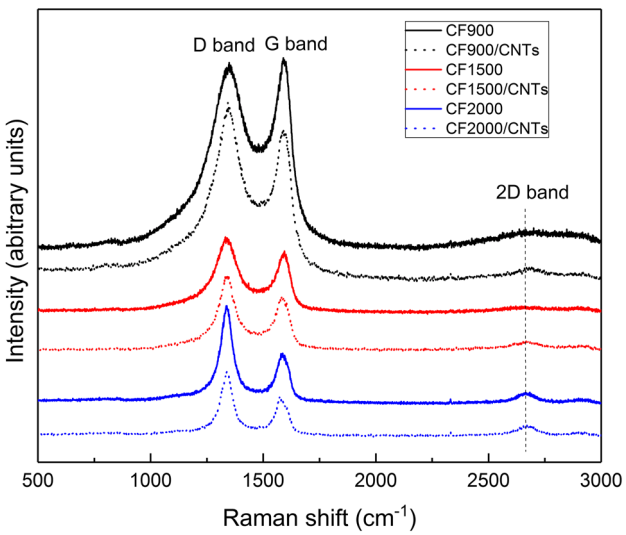

Figure 5 Typical Raman spectra for CF900, CF900/CNTs, CF1500, CF1500/CNTs, CF2000 and CF2000/CNTs samples.

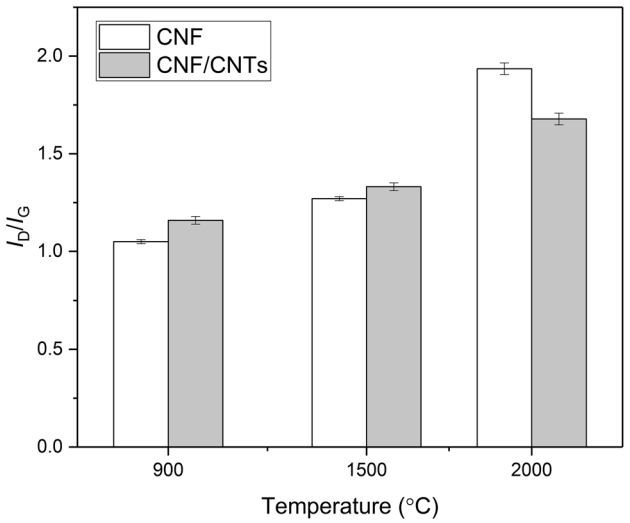

Figure 6 Intensity ratio of D band and G band, I_D/I_G, for CNF and CNF/CNTs.

bonds which in turn improves mechanical properties and electrical resistivity [27]. The I_D/I_G value, however, decreases from 1.94 ± 0.03 to 1.68 ± 0.03 for CF2000 with the growth of CNTs, in accordance with an increase in the L_a value from 2.56 ± 0.04 to 2.95 ± 0.05 nm, following Eq. 2. This increase indicates an improved degree of graphitization after the growth of CNTs on the CF2000 sample. Moreover, the presence of a 2D Raman band is noted at ~ 2700 cm^{-1} for the spectrum obtained from the CF900/CNTs, CF1500/CNTs, CF2000, and CF2000/CNTs samples. This band is absent for the CF900 and CF1500 samples, indicating that the 2D band is derived from either the CNTs on the surfaces of CF900 and CF1500, or also the highly graphitized fibres produced at higher temperatures (> 1600 °C). It is noted that the 2D Raman band is also observed for the CF2000 sample, indicating that a graphitized structure is well developed at 2000 °C. The I_{2D}/I_D ratios have been recorded for the CF900/CNTs, CF1500/CNTs, and CF2000/CNTs samples, and found to be 0.053 (0.001), 0.093 (0.002) and 0.149 (0.003) (errors are negligible and quoted in brackets), respectively. The I_{2D}/I_D ratio increases with an increase of the carbonization temperature, suggesting a reduction in structural defects [28]. It is also noted that the I_{2D}/I_D ratio increases when the growth of CNTs occurs on the CF2000 sample; from 0.096 (0.002) to 0.149 (0.003) (errors are negligible and quoted in brackets). This suggests that the growth of CNTs increases the crystallinity of the CF2000 sample.

In situ deformation studies

The presence of a shift in the G band for a deformed composite sample would indicate a stress transfer taking place between the resin and the fibres. No obvious Raman shifts were observed for the CF900, CF900/CNTs, CF1500, and CF1500/CNTs samples (Fig. 7a–d). This is due to the fact that the graphitic structures are not well developed at carbonization temperatures up to 1500 °C [23]. Beyond these temperatures, it is thought that a more well-developed and graphitized structure is formed, leading to higher mechanical properties of the fibres, and thereby better stress transfer properties.

Shifts in the position of the G band were however observed for the CF2000 and CF2000/CNTs samples (Fig. 8), indicating that stress has transferred between the matrix and the fibres. Shift rates with respect to strain $(d(\Delta\nu)/d\varepsilon)$ of − 4.5 and − 8.4 cm^{-1} $\%^{-1}$ are found for CF2000 and CF2000/CNTs, respectively. Young's modulus of the fibres can be estimated using the equation

$$E = \frac{d\sigma}{d(\Delta\nu)} \times \frac{d(\Delta\nu)}{d\varepsilon} = \frac{d\sigma}{d\varepsilon} \quad (3)$$

where E is the Young's modulus. The stress sensitivity of the Raman band shift is expressed by $(d(\Delta\nu)/d\sigma)$, where $\Delta\nu$ is the value of the Raman band shift and σ is the stress. The value of stress sensitivity of the Raman band shift for the G band emanating from carbon fibres and graphene has been found to be − 3.1 cm^{-1}/GPa [29]. The moduli for CF2000 and CF2000/CNTs are therefore estimated to be ~ 145 and ~ 271 GPa, respectively. These moduli are comparable to other electrospun cellulose-based carbon fibres (~ 100 GPa; [6]). Given this stress transfer from the matrix to the fibres and that they have intrinsically high mechanical stiffness, these materials are thought to be suitable for structural supercapacitors.

Discussion

Structural supercapacitors rely on the combination of high mechanical properties and electrocapacitive performance of the materials used for their construction. The main component of a structural supercapacitor is the electrode material, which should possess both sufficient electrical conductivity

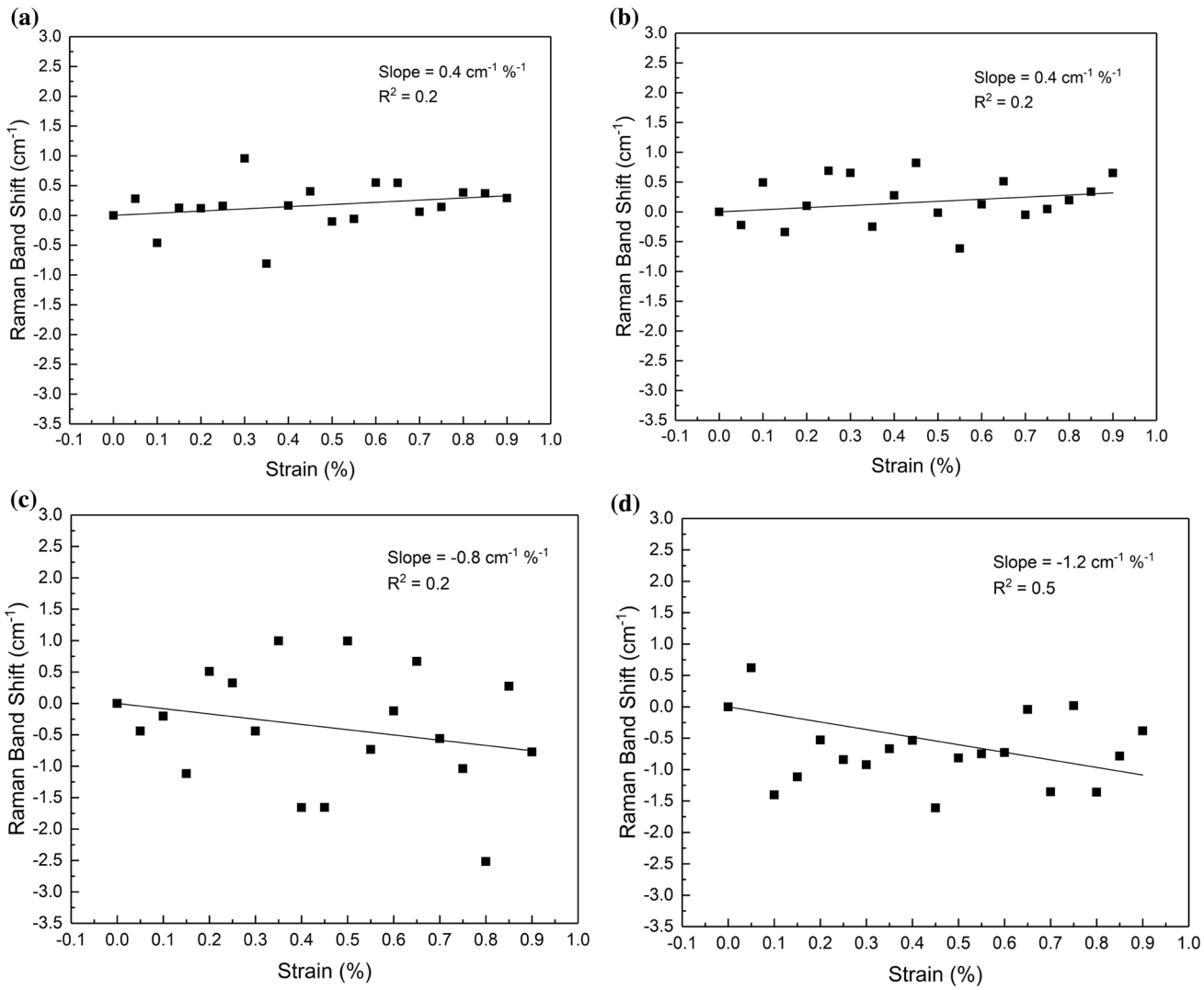

Figure 7 Typical plots of Raman band shift versus strain for **a** CF900, **b** CF900/CNTs, **c** CF1500 and **d** CF1500/CNTs samples, with linear regressions to the data (black line).

and high mechanical properties. As laminated carbon fibre composites have a similar architecture to supercapacitors, woven carbon fibres have been chosen as electrodes for the fabrication of structural supercapacitors in recent years [20, 30]. In order to further improve their performance, the incorporation of woven carbon fibres with a carbon aerogel, has been attempted to increase the electrodes' surface area and pore volume [12].

It is important to note that the individual functionalities of a structural supercapacitor (mechanical and electrocapacitive performance) do not need to be better than the mono-functionality provided by conventional materials, but a compromise should be considered to achieve the system mass savings and energy efficiencies required [4]. The capacitive performance is generally not 'state-of-the-art' for structural supercapacitors, mainly because of the high resistance of the electrolyte matrix. Despite this, the capacitances of our electrode materials are still comparable with other recent studies [12, 30]. It is important to note that to maximize the mechanical properties of the composite, a stiff matrix is required to give sufficient stress transfer to the fibres. The matrix stiffness typically increases with an increase in the degree of cross-linking [31]. This stiffening of the matrix, for one containing polymer electrolytes, will then reduce the mobility of the ions, and therefore reduce conductivity. In this sense, these two properties work against each other. Javaid et al. reported

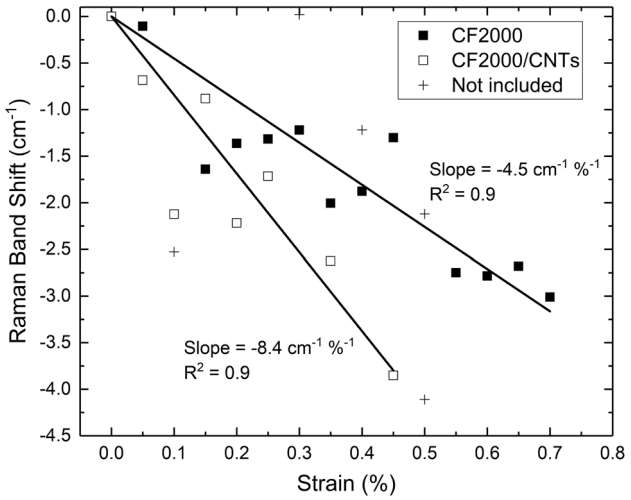

Figure 8 Shift in the position of the G band as a function of strain for CF2000 and CF2000/CNTs samples. + − data not included in the fit.

that an increase in the EMITFSI concentration results in increased ionic conductivity but decreased compression strength of PEGDGE electrolytes [30]. Similarly, in our study, the increased R_s at 24 h compared to 2 h of curing of the electrolyte matrix also suggested that the higher degree of cross-linking is not good for the electrocapacitive performance. Therefore, in real applications, the concentration of ILs in the electrolyte matrix should be adjusted to balance the multifunctionality of the structural supercapacitor. This balance can be also achieved by using alternative electrolyte matrices, such as polyethylene glycol (PEG) [32], polyethylene-oxide (PEO) [33], or a diglycidylether of bisphenol-A (DGEBA) [34]. Electrical conductivity increases for carbon fibres produced at higher temperatures [35]; the CF2000 sample is therefore expected to have an increased conductivity compared to CF900, and therefore improved capacitive properties. This means that there is also potentially an advantage to processing higher stiffness fibres for capacitive properties. Structural supercapacitor research is still at a very early stage. New electrodes and electrolyte matrices that can achieve both high mechanical and electrical properties are yet to be discovered. Therefore, we must pursue further work to address finding an optimum between mechanical and electrocapacitive performance.

Conclusions

Structural supercapacitors have been fabricated by using CNF decorated with CNTs as electrodes. A solid resin (PEGDGE) and an ionic liquid (EMITFSI) electrolyte were used. Capacitive properties of these devices have been measured. CF900/CNTs electrode-based capacitors exhibited a higher capacitive performance than CF900 electrodes (cf. 0.91 ± 0.02 and 3.35 ± 0.05 mF cm^{-2}). There was a decrease in this performance with increased curing time of the resin, from 2 to 24 h, due to a lack of charge carrier mobility in the latter samples. An in situ Raman spectroscopic study was used to investigate the stress transfer between a resin and the CNF and CNF/CNTs samples. Shifts were observed for the CF2000 and CF2000/CNTs samples. These shifts were then used to estimate the moduli of these samples, which were found to be $\sim$ 145 and $\sim$ 271 GPa, respectively. This result indicates that these electrospun cellulose-based CNF have potential as electrodes for the fabrication of structural supercapacitors.

Acknowledgements

The authors thank the Chinese Scholarship Council and the University of Exeter for funding a studentship (for Q. L.).

References

[1] Gonzalez E, Goikolea E, Barrena JA, Mysyk R (2016) Review on supercapacitors: technologies and materials. Renew Sustain Energy Rev 58:1189–1206

[2] Salanne M, Rotenberg B, Naoi K, Kaneko K, Taberna PL, Grey CP, Dunn B, Simon P (2016) Efficient storage mechanisms for building better supercapacitors. Nat Energy 1:16070

[3] Deka BK, Hazarika A, Kim J, Park YB, Park HW (2017) Recent development and challenges of multifunctional structural supercapacitors for automotive industries. Int J Energy Res 41:1397–1411

[4] Qian H, Diao H, Shirshova N, Greenhalgh ES, Steinke JG, Shaffer MS, Bismarck A (2013) Activation of structural carbon fibres for potential applications in multifunctional structural supercapacitors. J Coll Interf Sci 395:241–248

[5] Zhang BA, Kang FY, Tarascon JM, Kim JK (2016) Recent advances in electrospun carbon nanofibers and their application in electrochemical energy storage. Prog Mater Sci 76:319–380

[6] Deng LB, Young RJ, Kinloch IA, Zhu YQ, Eichhorn SJ (2013) Carbon nanofibres produced from electrospun cellulose nanofibres. Carbon 58:66–75

[7] Deng L, Young RJ, Kinloch IA, Abdelkader AM, Holmes SM, De Haro-Del Rio DA, Eichhorn SJ (2013) Supercapacitance from cellulose and carbon nanotube nanocomposite fibers. ACS Appl Mater Interfaces 5:9983–9990

[8] Li Q, Deng LB, Kim JK, Zhu YQ, Holmes SM, Perez-Page M, Eichhorn SJ (2017) Growth of carbon nanotubes on electrospun cellulose fibers for high performance supercapacitors. J Electrochem Soc 164:A3220–A3228

[9] Jin S-Y, Young RJ, Eichhorn SJ (2014) Controlling and mapping interfacial stress transfer in fragmented hybrid carbon fibre–carbon nanotube composites. Compos Sci Technol 100:121–127

[10] Jin S-Y, Young RJ, Eichhorn SJ (2014) Hybrid carbon fibre–carbon nanotube composite interfaces. Compos Sci Technol 95:114–120

[11] Schadler LS, Giannaris SC, Ajayan PM (1998) Load transfer in carbon nanotube epoxy composites. Appl Phys Lett 73:3842–3844

[12] Qian H, Kucernak AR, Greenhalgh ES, Bismarck A, Shaffer MS (2013) Multifunctional structural supercapacitor composites based on carbon aerogel modified high performance carbon fiber fabric. ACS Appl Mater Interfaces 5:6113–6122

[13] Papageorgiou DG, Kinloch IA, Young RJ (2017) Mechanical properties of graphene and graphene-based nanocomposites. Prog Mater Sci 90:75–127

[14] Huang Y, Young RJ (1995) Effect of fibre microstructure upon the modulus of PAN- and pitch-based carbon fibres. Carbon 33:97–107

[15] Prabhakaran K, Stephen JE, Robert JY (2007) Deformation of isolated single-wall carbon nanotubes in electrospun polymer nanofibres. Nanotechnology 18:235707

[16] Mohiuddin TMG, Lombardo A, Nair RR, Bonetti A, Savini G, Jalil R, Bonini N, Basko DM, Galiotis C, Marzari N, Novoselov KS, Geim AK, Ferrari AC (2009) Uniaxial strain in graphene by Raman spectroscopy: G peak splitting, Gruneisen parameters, and sample orientation. Phys Rev B 79:205433

[17] Xu P, Loomis J, Panchapakesan B (2012) Load transfer and mechanical properties of chemically derived single layer graphene reinforcements in polymer composites. Nanotechnology 23:505713

[18] Andrews R, Jacques D, Qian D, Rantell T (2002) Multiwall carbon nanotubes: synthesis and application. Acc Chem Res 35:1008–1017

[19] Hudak NS, Schlichting AD, Eisenbeiser K (2017) Structural supercapacitors with enhanced performance using carbon nanotubes and polyaniline. J Electrochem Soc 164:A691–A700

[20] Shirshova N, Qian H, Shaffer MSP, Steinke JHG, Greenhalgh ES, Curtis PT, Kucernak A, Bismarck A (2013) Structural composite supercapacitors. Compos A Appl Sci Manuf 46:96–107

[21] Hung KS, Masarapu C, Ko TH, Wei BQ (2009) Wide-temperature range operation supercapacitors from nanostructured activated carbon fabric. J Power Sour 193:944–949

[22] Li Y, Zhang Q, Zhang J, Jin L, Zhao X, Xu T (2015) A top-down approach for fabricating free-standing bio-carbon supercapacitor electrodes with a hierarchical structure. Sci Rep 5:14155

[23] Kong K, Deng LB, Kinloch IA, Young RJ, Eichhorn SJ (2012) Production of carbon fibres from a pyrolysed and graphitised liquid crystalline cellulose fibre precursor. J Mater Sci 47:5402–5410. https://doi.org/10.1007/s10853-012-6426-y

[24] Ferrari AC, Robertson J (2000) Interpretation of Raman spectra of disordered and amorphous carbon. Phys Rev B 61:14095–14107

[25] Matthews MJ, Pimenta MA, Dresselhaus G, Dresselhaus MS, Endo M (1999) Origin of dispersive effects of the Raman D band in carbon materials. Phys Rev B 59:R6585–R6588

[26] Tuinstra F, Koenig JL (1970) Raman spectrum of graphite. J Chem Phys 53:1126–1130

[27] Pimenta MA, Dresselhaus G, Dresselhaus MS, Cancado LG, Jorio A, Saito R (2007) Phys Chem Chem Phys 9:1276–1291

[28] McKee GS, Vecchio KS (2006) Thermogravimetric analysis of synthesis variation effects on CVD generated multiwalled carbon nanotubes. J Phys Chem B 110:1179–1186

[29] Frank O, Tsoukleri G, Riaz I, Papagelis K, Parthenios J, Ferrari AC, Geim AK, Novoselov KS, Galiotis C (2011) Nat Commun 2:255

[30] Javaid A, Ho KKC, Bismarck A, Steinke JHG, Shaffer MSP, Greenhalgh ES (2016) Carbon fibre-reinforced poly(ethylene glycol) diglycidylether based multifunctional structural

supercapacitor composites for electrical energy storage applications. J Compos Mater 50:2155–2163

[31] Gonzalez C, Vilatela JJ, Molina-Aldareguia JM, Lopes CS, Lorca JL (2017) Structural composites for multifunctional applications: current challenges and future trends. Prog Mater Sci 89:194–251

[32] Snyder JF, Gienger EB, Wetzel ED (2015) Performance metrics for structural composites with electrochemical multifunctionality. J Compos Mater 49:1835–1848

[33] Westover AS, Shabab FN, Tian JW, Bernath S, Oakes L, Erwin WR, Carter R, Bardhan R, Pint CL (2014) Stretching ion conducting polymer electrolytes: in-situ correlation of mechanical, ionic transport, and optical properties. J Electrochem Soc 161:E112–E117

[34] Javaid A, Ho KKC, Bismarck A, Shaffer MSP, Steinke JHG, Greenhalgh ES (2013) Multifunctional structural supercapacitors for electrical energy storage applications. J Compos Mater 48:1409–1416

[35] Minus M, Kumar S (2005) The processing, properties, and structure of carbon fibers. JOM 57:52–58